Dielectric properties of $LiTaO_3$

Izumi Tomeno
Toshiba Research and Development Center, Toshiba Corporation, Saiwai-ku, Kawasaki 210, Japan

Sadao Matsumura
Electron Tube and Device Division, Toshiba Corporation, Saiwai-ku, Kawasaki 210, Japan
(Received 20 November 1987)

The dielectric susceptibilities χ_{ii} and conductivities σ_{ii} in $LiTaO_3$ are measured over a broad temperature range up to 1200 K at frequencies up to 13 MHz. The dielectric properties are compared with previously published results on the elastic properties. Both the inverse-susceptibility difference between constant strain and constant stress $(\chi_{ii}^x)^{-1}-(\chi_{ii}^X)^{-1}$ and the elastic-constant difference between constant polarization and constant field $C_{ii}^P-C_{ii}^E$ are interpreted consistently in terms of both electrostrictive and higher-order interactions between the strain and polarization. The contribution of higher-order interactions to $(\chi_{33}^x)^{-1}-(\chi_{33}^X)^{-1}$ and $C_{33}^P-C_{33}^E$ appears to be attributable to anharmonicity in the soft mode. Both χ_{33} and σ_{33} exhibit significant dispersion over a wide temperature range, including $T_C=868$ K. This may be related with vacancies or Li ion motion. A comparison with light-scattering measurements suggests that the phase transition in $LiTaO_3$ has an intermediate character between the displacive and order-disorder categories.

I. INTRODUCTION

Lithium tantalate ($LiTaO_3$) and lithium niobate ($LiNbO_3$) undergo only a single structural phase transition, from the low-temperature ferroelectric (FE) phase to the high-temperature paraelectric (PE) phase. The FE phase has a crystal structure with $R3c$ space-group symmetry and the PE phase has the centrosymmetric space group $R\bar{3}c$. The Curie temperature T_C is 870 K for $LiTaO_3$ and 1210 K for $LiNbO_3$. The crystal structures and optical properties of these materials have been studied extensively in order to elucidate the mechanism of the phase transition.[1-9] There is still considerable uncertainty concerning the characters of the phase transitions in $LiTaO_3$ and $LiNbO_3$.

Neutron scattering results support the concept that the phase transition in $LiTaO_3$ and $LiNbO_3$ has order-disorder character involving the Li atoms. Abrahams *et al.*[1] made neutron scattering measurements on $LiTaO_3$ and interpreted them to mean that Li atoms above T_C occupy two equivalent positions on either side of the oxygen plane with equal probability. Samuelsen and Grande[2] studied the neutron diffraction in $LiTaO_3$ below T_C and explained the spontaneous polarization in terms of the gradual ordering of Li atoms as the temperature decreases. Chowdhury *et al.*[3] investigated the phonon dispersion curves in $LiNbO_3$ by inelastic neutron scattering and showed that there is no evidence of the softening of the A_1 mode at temperatures up to $0.6T_C$.

In contrast to the neutron results, light-scattering measurements have established the existence of the soft mode. Johnston and Kaminow[4] studied the Raman spectra in two crystals and found the A_1 mode, whose frequency varies approximately as $(T_C-T)^{0.5}$ below T_C. In the case of $LiTaO_3$, Penna *et al.*[5,6] reported a diffusive central mode in Raman spectra and an anomalous polariton dispersion curve. They suggested that dynamical domain fluctuations occur below T_C in $LiTaO_3$. Müller *et al.*[7] deduced the temperature dependence of the soft-mode frequency in $LiTaO_3$ from infrared-reflectivity data and found that the soft-mode frequency remains finite in the vicinity of T_C. Zhang and Scott[8] measured the Raman spectra in $LiTaO_3$ and found that the soft mode becomes overdamped and couples with the relaxation process at temperatures far lower than T_C. A similar conclusion has been obtained from Raman spectra in $LiNbO_3$ by Okamoto *et al.*[9]

Recently, Tomeno and Matsumura[10] reported elastic and dielectric constants in $LiNbO_3$, and explained these data consistently in terms of the interaction between strain and polarization. Furthermore, they found dielectric dispersion above T_C in the frequency range between 1 and 13 MHz. In the case of $LiTaO_3$, the temperature dependence of the dielectric constant ϵ_{33} was determined at frequencies up to 20 kHz. Glass[11] and Yamada *et al.*[12] observed that the constant-stress dielectric constant ϵ_{33}^x obeys a Curie-Weiss law. Prieto *et al.*[13] measured the frequency dependence of the dielectric constant ϵ_{33} in the PE phase of $LiTaO_3$ up to 10 MHz and concluded that defects contribute to the low-frequency dielectric dispersion. Previously, Tomeno[14] investigated elastic constants C_{ii} in $LiTaO_3$ as a function of temperature up to 973 K. In addition to the elastic-constant data, constant-strain dielectric constant data are highly necessary in order to understand the phase-transition mechanism in $LiTaO_3$.

In this paper we present the temperature dependence of dielectric constants ϵ_{ii} and electric conductivities σ_{ii} in $LiTaO_3$ at frequencies up to 13 MHz. We analyze the present ϵ_{ii} results and the previous C_{ii} results using a phe-

nomenological expression. We report the marked dispersion in ϵ_{ii} and σ_{ii} at temperatures near T_C. The dielectric results for $LiTaO_3$ are compared with those for $LiNbO_3$, and are discussed in relation with soft-mode behavior observed by the light-scattering experiments.

II. EXPERIMENTAL PROCEDURE

Dielectric constant ϵ_{ii} and electric conductivity σ_{ii} were determined at several frequencies, between 10 kHz and 13 MHz, using a Yokokawa Hewlett Packard impedance analyzer 4192 A.

Samples used in the present investigation were cut from $LiTaO_3$ crystals with congruent melt composition. These crystals were grown using the Czochralski technique from a Pt-Rh crucible, which inevitably causes contamination by Rh impurities for an approximately 100 ppm concentration. Comparison with ϵ_{ii} for high-purity $LiTaO_3$ crystal revealed that the Rh impurity exerts no influence on the dielectric constant in $LiTaO_3$.

Single-domain (SD) crystals were obtained by field cooling as-grown crystals with a 5-V/cm electric field applied along the Z axis through T_C. They were shaped into plates, 16 to 25 mm^2 in area and 1.0 to 1.2 mm in thickness. The SD sample, with platinum electrodes on large-Z faces, was prepared for measuring ϵ_{33} and σ_{33}. The multidomain (MD) sample, with platinum electrodes on Y surfaces, was used for measuring ϵ_{11} above T_C, while the SD sample, with gold electrodes, was prepared for measuring ϵ_{11} below T_C. Platinum electrodes were made of fritless platinum paste, fired at 1000 K in the initial warm up. Gold electrodes were vapor deposited in a vacuum, and then covered with gold paste and fired at 800 K. Capacitance measurements on the thicker sample yielded the same ϵ_{ii} value over the entire temperature range. The measured data were not affected by the boundary between the electrodes and crystal.

III. RESULTS

Figure 1 indicates dielectric constants ϵ_{11} and ϵ_{33} in $LiTaO_3$ as a function of temperature. Except for the high-temperature range, the measured ϵ_{ii} values up to 1.5 MHz represent the constant-stress dielectric constants ϵ_{ii}^X, while the values at 10 and 13 MHz represent the constant-strain dielectric constants ϵ_{ii}^x.

At room temperature, the dielectric-constant difference $\epsilon_{11}^X - \epsilon_{11}^x$ in $LiTaO_3$ is small compared with that in $LiNbO_3$.[10] Both constant-stress and constant-strain dielectric constants ϵ_{11} increase gradually with increasing temperature. They exhibit a maximum at T_C and then decrease slowly in the PE phase. Dielectric dispersion, perpendicular to the Z axis, is observed in the PE phase, where the crystal is centrosymmetric.

The dielectric-constant difference $\epsilon_{33}^X - \epsilon_{33}^x$ in $LiTaO_3$ at room temperature is much less than $\epsilon_{11}^X - \epsilon_{11}^x$. The relationship $(\epsilon_{33}^X - \epsilon_{33}^x) \ll (\epsilon_{11}^X - \epsilon_{11}^x)$ is also found in $LiNbO_3$ at temperatures far lower than T_C.[10] Note that there is a significant dispersion in ϵ_{33} over the wide temperature range, including the Curie temperature.

Relative inverse dielectric susceptibility χ_{33}^{-1} is plotted in Fig. 2 as a function of temperature. The lowest-

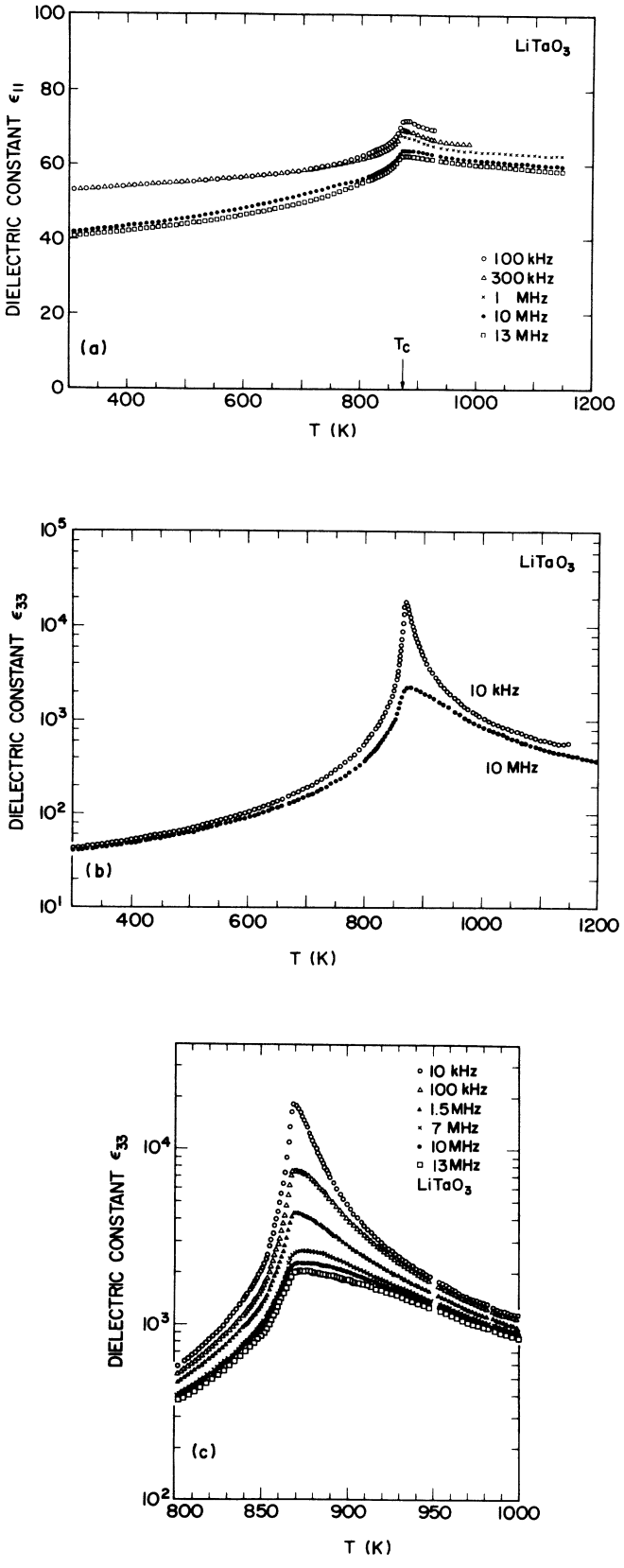

FIG. 1. Temperature dependence of dielectric constants ϵ_{ii} in $LiTaO_3$. (a) ϵ_{11} along the Y axis. (b) ϵ_{33} along the Z axis. (c) Details of ϵ_{33} near T_C.

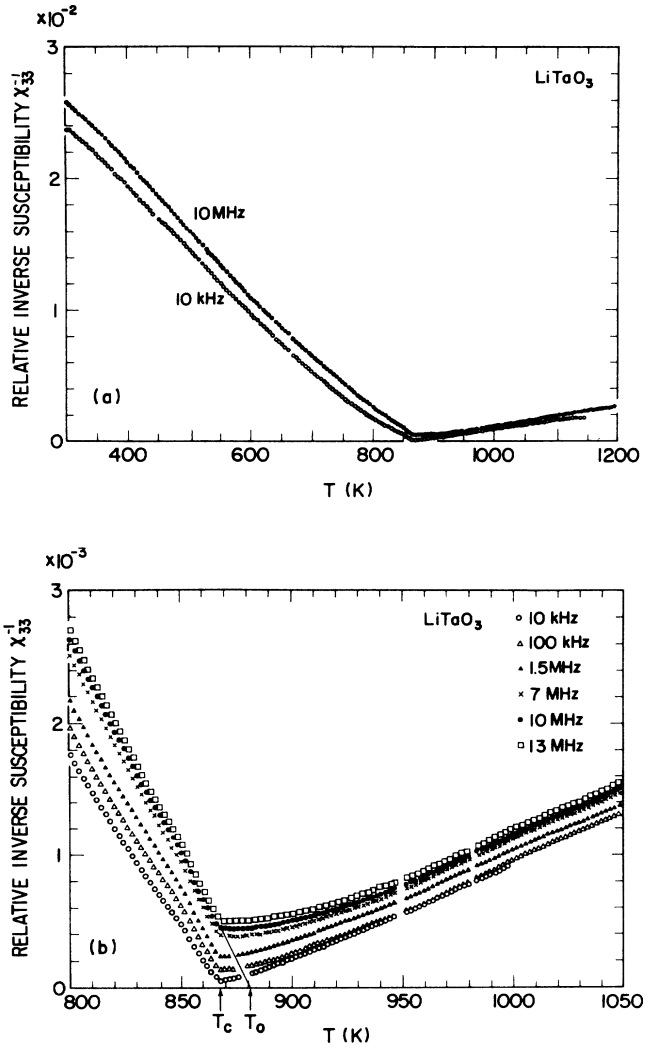

FIG. 2. Inverse dielectric susceptibility χ_{33}^{-1} in $LiTaO_3$. (a) χ_{33}^{-1} as a function of temperature up to 1200 K. (b) Details of χ_{33}^{-1} near $T_C = 868$ K. Note that χ_{33}^{-1} shows dispersion in the PE phase.

frequency inverse susceptibility $(\chi_{33}^X)^{-1}$ in the PE phase clearly obeys the Curie-Weiss behavior

$$(\chi_{33}^X)^{-1}=(T-T_C)/C^+, \quad T>T_C \ , \tag{1}$$

where C^+ is the Curie constant above T_C. As indicated in Fig. 2(b), in the FE phase $(\chi_{33}^X)^{-1}$ at 10 kHz shows the linear temperature dependence and is described by a modified Curie-Weiss relation:

$$(\chi_{33}^X)^{-1}=(T_C-T)/C^-, \quad T<T_C \ , \tag{2}$$

where C^- is the Curie constant below T_C. The Curie temperature T_C in the $LiTaO_3$ sample used for dielectric measurements is 868 K and agrees with the value for the congruent melt composition reported by Barns and Carruthers.[15] The slope for $(\chi_{33}^X)^{-1}$ at 10 kHz in the PE phase yields a Curie constant of $C^+=1.43\times10^5$ K, which is in good agreement with the value reported by Yamada *et al.*[12] and by Glass.[11] The ratio of Curie constants C^+/C^- for $LiTaO_3$ at 10 kHz is 2.7 and agrees well with that for $LiNbO_3$, although the C^+ value for $LiNbO_3$ is only half as large as that for $LiTaO_3$.[10]

High-frequency inverse susceptibility $(\chi_{33}^x)^{-1}$ in the PE phase decreases linearly with decreasing temperature, deviates from linearity, and then becomes practically constant with temperature in the neighborhood of T_C. In the range between 950 and 1200 K, the slopes for $(\chi_{33}^X)^{-1}$ at 10 and 100 kHz are equal to the slopes for $(\chi_{33}^x)^{-1}$ at 10 and 13 MHz. In the FE phase, $(\chi_{33}^x)^{-1}$ at 10 MHz decreases linearly with increasing temperature. When extrapolated, it crosses the abscissa at $T_0=881$ K, 13 K higher than T_C [see Fig. 2(b)]. Below T_C, $(\chi_{33}^x)^{-1}$ at 10 MHz is expressed as

$$(\chi_{33}^x)^{-1}=(T_0-T)/C'^-, \quad T<T_C \ , \tag{3}$$

where C'^- is the modified Curie constant below T_C.

As shown in Fig. 3, the conductivity σ_{33} along the Z axis exhibits a maximum at T_C. In addition, σ_{33} shows significant dispersion over the wide temperature range between 700 and 1200 K. The conductivity σ_{33} increases with increasing frequency. As indicated in Fig. 3(b), variations of σ_{11} with frequency near T_C are far less than those of σ_{33}. The conductivity σ_{11} increases with increasing temperature, up to 1150 K. The lowest-frequency conductivity σ_{33} shows similar temperature dependence, with the exception of the anomalous part associated with the phase transition. A plot of $\log_{10}\sigma_{11}$ versus $1/T$ in Fig. 3(c) suggests that σ_{11} varies approximately as $\exp(-Q/kT)$ with $Q=1.1$ eV.

IV. DISCUSSION

A. Phenomenological interpretation

In order to discuss our susceptibility and elastic-constant experiments, we use a phenomenological expression of the lattice free energy $F(x_m,P_i)$ involving strain x_m and polarization P_i. The free energy $F(x_m,P_i)$ for $LiTaO_3$ is written as

$$F(x_m,P_i)=F_m(x_m)+F_0(P_i)+F_C(x_m,P_i) \ , \tag{4}$$

$$\begin{aligned}F_m(x_m)=&\tfrac{1}{2}C_{11}^P(x_1^2+x_2^2)+\tfrac{1}{2}C_{33}^P x_3^2+\tfrac{1}{2}C_{44}^P(x_4^2+x_5^2)\\&+\tfrac{1}{2}C_{66}^P x_6^2+C_{12}^P x_1x_2+C_{13}^P(x_1+x_2)x_3\\&+C_{14}^P[(x_1-x_2)x_4+x_5x_6] \ ,\end{aligned} \tag{5}$$

$$F_0(P_i)=\tfrac{1}{2}\chi_{11}^{-1}(P_1^2+P_2^2)+\tfrac{1}{2}\chi_{33}^{-1}P_3^2+\tfrac{1}{4}AP_3^4 \ , \tag{6}$$

$$\begin{aligned}F_C(x_i,P_m)=&q_{33}x_3P_3^2+q_{14}[(x_1-x_2)P_2+x_6P_1]P_3\\&+q_{44}(x_4P_2+x_5P_1)P_3\\&+r_{333}x_3P_3^4+[r_{134}(x_1-x_2)+r_{344}x_4]P_2P_3^3\\&+(r_{344}x_5+r_{356}x_6)P_1P_3^3 \ .\end{aligned} \tag{7}$$

Here, $F_m(x_m)$ refers to the elastic-strain energy and $F_0(P_i)$ represents the Landau free-energy expansion, with respect to polarization alone. For simplicity, terms

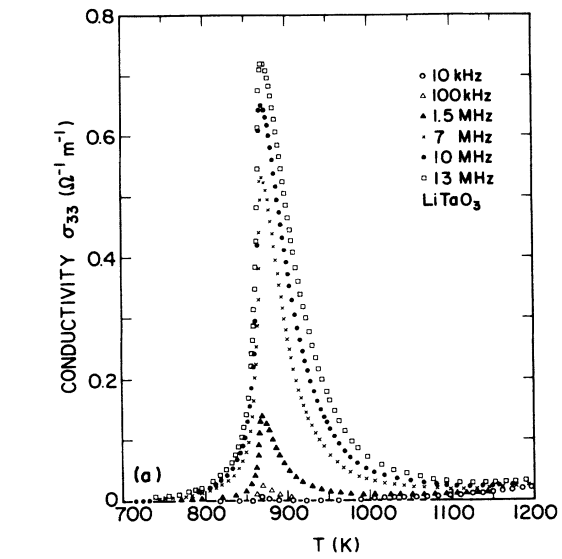

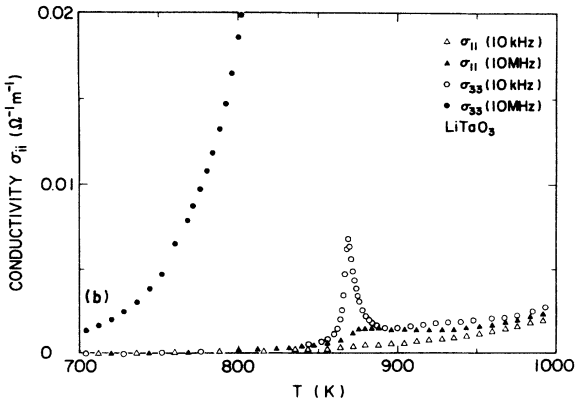

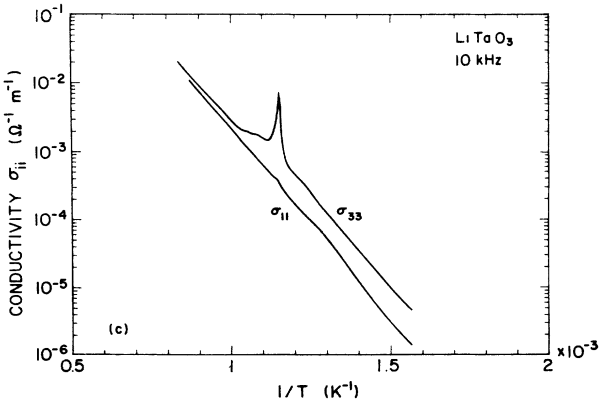

FIG. 3. Conductivity σ_{ii} in $LiTaO_3$. (a) Temperature and frequency dependence of σ_{33}. (b) σ_{11} and σ_{33} at 10 kHz and 10 MHz as a function of temperature. (c) σ_{11} and σ_{33} at 10 kHz as a function of reciprocal temperature.

higher than P_3^6 are dropped in Eq. (6) and the coefficient A is assumed to be a constant. Free interaction energy $F(x_C, P_m)$ arises from the coupling between strain and polarization. Since the piezoelectric coupling term axP is forbidden by symmetry above T_C, the lowest-order interaction in the PE phase is the electrostrictive coupling of the form qxP^2. In addition, we take into account higher-order coupling of the form rxP^4, to interpret the temperature dependence of $(\chi_{ii}^x)^{-1}-(\chi_{ii}^X)^{-1}$ and $C_{ii}^P-C_{ii}^E$. In the FE phase, the spontaneous polarization P_s induces piezoelectric coupling axP. For $LiTaO_3$ the piezoelectric constant a_{31} value is approximately zero at room temperature.[16] Therefore, Eq. (7) neglects q_{13} related with $a_{31}=(\partial^2 F_C/\partial x_1 \partial P_3)$. Moreover, we exclude the terms hx^2P^2, because C_{33}^P has a linear temperature dependence with the same slopes on either side of T_C.[14] Thus the inverse-susceptibility difference $(\chi_{ii}^x)^{-1}-(\chi_{ii}^X)^{-1}$ and elastic-constant difference $C_{ii}^P-C_{ii}^E$ are expressed as[10]

$$(\chi_{11}^x)^{-1}-(\chi_{11}^X)^{-1}=2(q_{14}+r_{134}P_s^2)^2P_s^2(S_{11}^P-S_{12}^P)+(q_{44}+r_{134}P_s^2)^2P_s^2S_{44}^P+4(q_{14}+r_{134}P_s^2)\times(q_{44}+r_{344}P_s^2)P_s^2S_{14}^P , \quad (8)$$

$$(\chi_{33}^x)^{-1}-(\chi_{33}^X)^{-1}=4(q_{33}+2r_{333}P_s^2)^2P_s^2S_{33}^P , \quad (9)$$

$$C_{11}^P-C_{11}^E=(q_{14}+r_{134}P_s^2)^2P_s^2\chi_{11}^x , \quad (10)$$

$$C_{33}^P-C_{33}^E=4(q_{33}+2r_{333}P_s^2)^2P_s^2\chi_{33}^x , \quad (11)$$

$$C_{44}^P-C_{44}^E=(q_{44}+r_{344}P_s^2)^2P_s^2\chi_{11}^x , \quad (12)$$

$$C_{66}^P-C_{66}^E=(q_{14}+r_{134}P_s^2)^2P_s^2\chi_{11}^x . \quad (13)$$

Here, q_{ij}, r_{ijk}, and the elastic compliance S_{ii}^P are assumed to be temperature independent. The assumption of S_{ii}^P is based on the fact that the relative temperature derivatives $(S_{ii}^E)^{-1}(dS_{ii}^E/dT)$ are of the order of 2×10^{-4} K^{-1}.[12] In the absence of r_{ijk}, Eqs. (8)–(13) predict that $(C_{ii}^P-C_{ii}^E)/\chi_{11}^X$, $(i=1,$ 4, and 6), $(C_{33}^P-C_{33}^E)/\chi_{33}^x$, $(\chi_{11}^x)^{-1}-(\chi_{11}^X)^{-1}$, and $(\chi_{33}^x)^{-1}-(\chi_{33}^X)^{-1}$ are proportional to P_s^2.

Figure 4 shows the temperature dependence of $(\chi_{mm}^x)^{-1}-(\chi_{mm}^X)^{-1}$ and $(C_{ii}^P-C_{ii}^E)/\chi_{mm}^x$ for $LiTaO_3$, deduced from the dielectric- and elastic-constant measurements. Except for near T_C, relative values for $(\chi_{11}^x)^{-1}-(\chi_{11}^X)^{-1}$ agree with those for $(C_{44}^P-C_{44}^E)/\chi_{11}^x$, while the values for $(\chi_{33}^x)^{-1}-(\chi_{33}^X)^{-1}$ agree with those for $(C_{33}^P-C_{33}^E)/\chi_{33}^x$. This correspondence is also found for $LiNbO_3$.[10] Following Eqs. (8)–(13), the temperature dependence of the inverse-susceptibility difference $(\chi_{mm}^x)^{-1}-(\chi_{mm}^X)^{-1}$ is compatible with that of the elastic-constant difference $C_{ii}^P-C_{ii}^E$. Relative values for $(\chi_{33}^x)^{-1}-(\chi_{33}^X)^{-1}$ and $(C_{33}^P-C_{33}^E)/\chi_{33}^x$ are lower than those for P_s^2, determined by Glass.[11] We tried to fit Eqs. (9) and (11) to the experimental data, using the ratio r_{333}/q_{33} as a free parameter. The solid line drawn in Fig. 4(b) is obtained with the P_s^2 data and $r_{333}/q_{33}=1.3$ m^4/C^2. The fit indicates that both $q_{33}x_3P_3^2$ and $r_{333}x_3P_3^4$ contribute to $(\chi_{33}^x)^{-1}-(\chi_{33}^X)^{-1}$ and $C_{33}^P-C_{33}^E$ in the wide

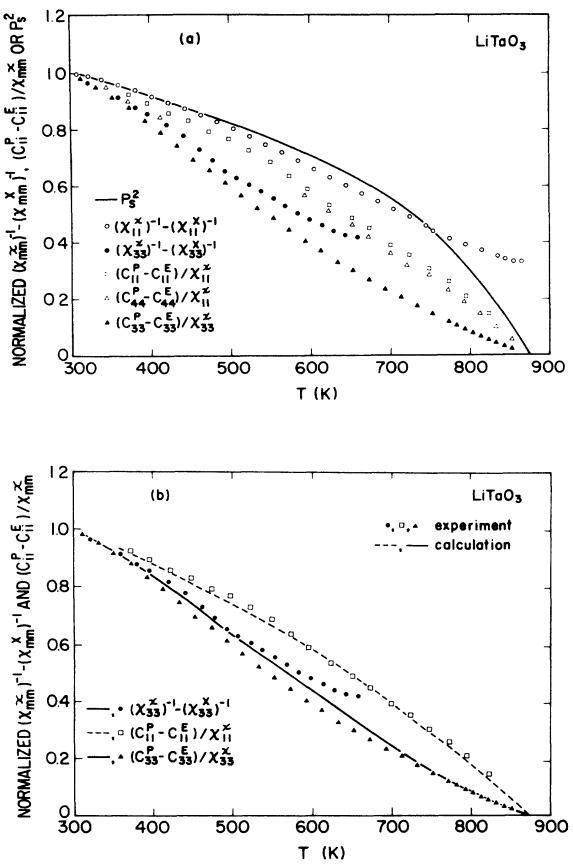

FIG. 4. Temperature dependence of $(C_{ii}^P - C_{ii}^E)/\chi_{mm}^x$, $(\chi_{mm}^x)^{-1} - (\chi_{mm}^X)^{-1}$, and P_s^2 for $LiTaO_3$. Each plot is normalized to unity at 300 K. (a) The experimental data. The C_{ii} and P_s^2 values are taken from Refs. 10 and 11, respectively. (b) Comparison with calculation. The solid and dashed lines are obtained from Eq. (11) with $r_{333}/q_{33} = 1.3$ m^4/C^2 and Eq. (10) with $r_{134}/q_{14} = 0.5$ m^4/C^2, respectively.

temperature range. We find the fit to the $(C_{11}^P - C_{11}^E)/\chi_{11}^x$ data in Fig. 4(b), using Eq. (12) with $r_{134}/q_{14} = 0.5$ m^2/C^4. The results suggest that the higher-order coupling of $r_{333}x_3P_3^4$ has an important effect on the dielectric and elastic properties of $LiTaO_3$, compared with the other rxP^4.

As shown in Fig. 4, both $(C_{33}^P - C_{33}^E)/\chi_{33}$ and P_s^2 vary approximately as $(T_C - T)$ in the vicinity of T_C, where the higher term $2r_{333}P_s^2$ is small, compared with q_{33}. In the framework of the Landau theory, the temperature variations of χ_{33}^x and P_s^2 cancel below T_C.[17] On the contrary, the cancellation is invalid for $\chi_{33}^x P_s^2$ in $LiTaO_3$. From the relation $P_s^2 \propto (T_C - T)$ and Eq. (3), the elastic-constant difference $C_{33}^P - C_{33}^E$ near T_C is given by

$$C_{33}^P - C_{33}^E = A\frac{T_C - T}{T_0 - T}, \quad T < T_C \ . \tag{14}$$

The Curie temperature T_C in the sample previously used for elastic measurements is 7 K higher than T_C in the sample for dielectric measurements. This may be explained from the fact that T_C is highly sensitive to the crystal composition.[15] In this analysis, we assume that $(\chi_{33}^x)^{-1}$ for the sample used for elastic measurement is expressed by Eq. (3) and that $T_0 - T_C$ is unaffected by the slight difference in T_C. The solid line in Fig. 5 is obtained from Eq. (14) with $A = 6.1 \times 10^9$ N/m^2, $T_C = 875$ K, and $T_0 = 888$ K. The good agreement indicates that the drastic change in $C_{33}^P - C_{33}^E$ between 800 K and T_C is attributed to the anomalous behavior of χ_{33}^x at high temperatures.

Spontaneous values for the strain x_{ms} and the polarization P_s are obtained by setting the stress X_m and the electric field E_3 equal to zero. The spontaneous strain x_{ms} values are expressed as

$$x_{1s} = x_{2s} = P_s^2(q_{33} + r_{333}P_s^2)C_{13}^P/\Delta C \ , \tag{15}$$

$$x_{3s} = -P_s^2(q_{33} + r_{333}P_s^2)(C_{11}^P + C_{12}^P)/\Delta C \ , \tag{16}$$

$$x_{4s} = x_{5s} = x_{6s} = 0 \ , \tag{17}$$

where

$$\Delta C = C_{33}^P(C_{11}^P + C_{12}^P) - 2(C_{13}^P)^2 \ . \tag{18}$$

In the FE phase of $LiTaO_3$, the lattice constant c exhibits anomalous temperature dependence, compared with the lattice constant a.[18] The significance of the higher-order interaction $r_{333}x_3P_3^4$ appears compatible with the estimation of spontaneous strain x_{is} in $LiTaO_3$ as reported by Yamada *et al.*[12] They revealed that a linear relationship between x_{3s} and P_s^2 is not valid at temperatures far lower than T_C and that the higher-order term P_s^4 contributes largely to the results for x_{is}. The spontaneous-strain ratio x_{3s}/x_{1s} is given by

$$\frac{x_{3s}}{x_{1s}} = -\frac{C_{11}^P + C_{12}^P}{C_{13}^P} \ . \tag{19}$$

The ratio $x_{3s}/x_{1s} = -3.5$, obtained from the C_{ij}^P data,[16] seems to be consistent with the results reported by Yamada *et al.*[12]

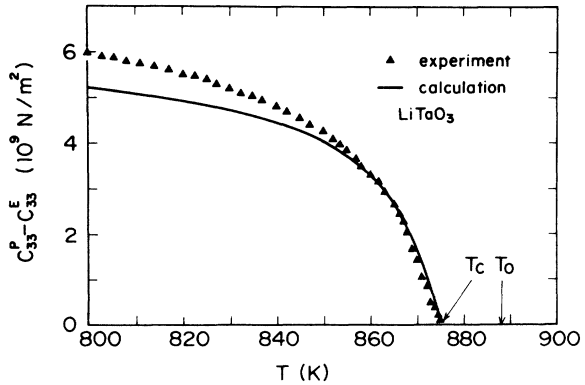

FIG. 5. Elastic-constant difference $C_{33}^P - C_{33}^E$ in $LiTaO_3$ as a function of temperature. The triangles show experimental results studied previously in Ref. 14. The solid line is obtained from Eq. (14) with parameters given in the text.

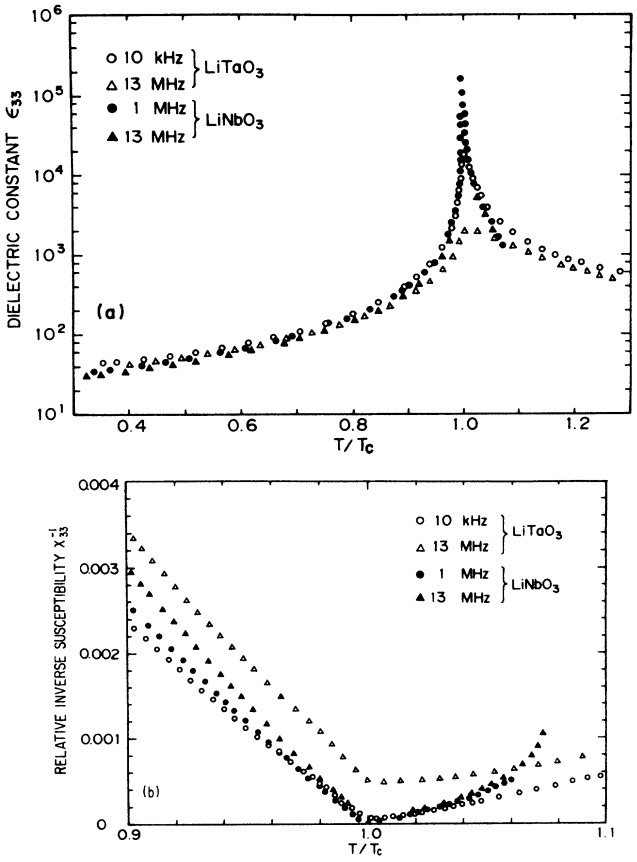

FIG. 6. Dielectric constants ϵ_{33} and inverse susceptibilities χ_{33}^{-1} in $LiTaO_3$ and $LiNbO_3$ as a function of reduced temperature T/T_C. The results for $LiNbO_3$ are taken from Ref. 10.

Inverse susceptibility $(\chi_{33}^x)^{-1}$ at constant strain is written as

$$(\chi_{33}^x)^{-1}=\chi_{33}^{-1}, \quad T>T_C \tag{20}$$

$$(\chi_{33}^x)^{-1}=-2\chi_{33}^{-1}+4P_s^2 q_{33} \times(q_{33}+r_{333}P_s^2)(C_{11}^P+C_{12}^P)/\Delta C, \quad T<T_C \ . \tag{21}$$

The second term in Eq. (21), derived from the interaction between strain and polarization, is smaller than the inverse-susceptibility difference $(\chi_{33}^x)^{-1}-(\chi_{33}^X)^{-1}$, given by Eq. (9). As shown in Fig. 2, in the PE phase, $(\chi_{33}^x)^{-1}$ increases linearly with increasing temperature in the range between 950 and 1200 K. In the FE phase $(\chi_{33}^x)^{-1}$ deviates slightly from linearity in the range T_C-250 K and T_C. The distinction between the two phases may be ascribed to the second term in Eq. (21).

Figure 6 shows ϵ_{33} and χ_{33}^{-1} in $LiTaO_3$ and $LiNbO_3$ as a function of reduced temperature T/T_C. In view of Eq. (1), Fig. 6(b) indicates that the C^+/T_C value for $LiTaO_3$ is nearly equal to that for $LiNbO_3$.

B. Comparison with light-scattering experiments

The constant-strain dielectric constants are connected with optical phonon frequencies by the generalized Lyddane-Sachs-Teller (LST) relation. As indicated in Table I, room-temperature clamped dielectric constants ϵ_{11}^x and ϵ_{33}^x, determined by this work, are in good agreement with the values for ϵ_{11}^x and ϵ_{33}^x, estimated from infrared reflection spectra[19] and from Raman scattering.[20] The inverse clamped dielectric susceptibility $(\chi_{33}^x)^{-1}$ is expected to be proportional to squared soft-mode frequency, obtained by light-scattering experiments. As shown in Fig. 7, the relative values for $(\chi_{33}^x)^{-1}$ are in good agreement with those for the square of intensity-weighted mean soft-mode frequency $\bar{\omega}^2$, deduced from the Raman spectra by Johnston and Kaminow.[4] At room temperature, the frequency of the soft A_1 mode is higher than frequencies of the other temperature-independent E modes. The soft mode couples with the E modes in succession with increasing temperature. The good agreement may be found by introducing the intensity-weighted soft mode.

Recently, Zhang and Scott[8] reexamined the Raman spectra in $LiTaO_3$. They assigned the broad peak centered at $\omega=0$ near T_C to the A_1 mode and interpreted that the soft A_1 mode is overdamped and coupled with the relaxation process at high temperatures. Their data were fitted using a response function

TABLE I. Dielectric constant values for $LiTaO_3$ at 293 K.

	Capacitance measurements Present work					Teague *et al.*[a]
f	10 kHz	100 kHz	1 MHz	10 MHz	13 MHz	1 GHz
ϵ_{11}	53.5	53.5		41.7	40.6	40.3
ϵ_{33}	42.4	42.2	42.0	39.2	38.8	41.4
	Infrared reflectivity Barker *et al.*[b]				Raman scattering Kaminow and Johnston[c]	
ϵ_{11}^x	41.5				41	
ϵ_{33}^x	37.6				43	

[a]J. R. Teague, R. R. Rice, and R. Gerson, J. Appl. Phys. **46**, 2864 (1975).
[b]Reference 19.
[c]Reference 20.

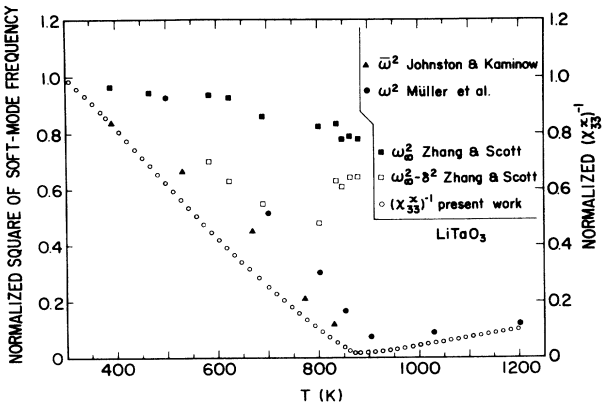

FIG. 7. Inverse susceptibility and squared soft-mode frequencies for $LiTaO_3$. Each plot is normalized to unity at 300 K. The triangles represent the mean-squared soft-mode frequency $\bar{\omega}^2$ determined by Johnston and Kaminow (Ref. 4). Open and solid squares denote ω_∞^2 and $\omega_\infty^2-\delta^2$, respectively, determined by Zhang and Scott (Ref. 8). Solid circles denote squared soft-mode frequency determined by Müller *et al.* (Ref. 7). Open circles refer to the constant-strain inverse susceptibility $(\chi_{33}^x)^{-1}$ by the present work.

$$G(\omega)=\left[\omega_\infty^2-\omega^2-i\omega\gamma-\frac{\delta^2}{1-i\omega\tau}\right]^{-1}, \tag{22}$$

where ω_∞ is the uncoupled soft-mode frequency, δ and τ denote the strength and characteristic time of the relaxation process coupled to the soft mode, respectively, and γ is the damping constant of the soft phonon. The soft-mode frequency squared ω_0^2, where $\omega_0^2=\omega_\infty^2-\delta^2$, is in disagreement with the inverse clamped susceptibility $(\chi_{33}^x)^{-1}$ at high temperatures, as indicated in Fig. 7. The reason for this discrepancy may be attributed to the underestimation for the δ^2 values near T_C. They pointed out that the parameter δ^2 is ambiguous, compared with effective coupling parameter $\delta^2\tau$.[8]

Müller *et al.*[7] deduced the soft-mode frequency in $LiTaO_3$ from infrared reflectivity data and found that its frequency remains finite at T_C. The coupling term δ^2 in Eq. (22) may contribute to the finite value for squared soft-mode frequency ω_0^2.

C. Dielectric dispersion

For $LiTaO_3$, both the dielectric constant ϵ_{33} and the conductivity σ_{33} show a marked dispersion over the wide temperature range, including T_C, as indicated in Figs. 1 and 3. Note that in Fig. 2(b) the difference in χ_{33}^{-1} between 10 kHz and 13 MHz is approximately independent of temperature above 950 K.

Frequency-dependent conductivity $\sigma_{ii}(\omega)$ is connected with the imaginary part of dielectric constant ϵ_{ii}'' as

$$\sigma_{ii}(\omega)=\epsilon_0\epsilon_{ii}''\omega\ . \tag{23}$$

In marked contrast to σ_{33}, σ_{11} is practically frequency independent, up to 13 MHz. For $LiTaO_3$ and $LiNbO_3$, the frequency-independent conductivity σ_{11} increases with

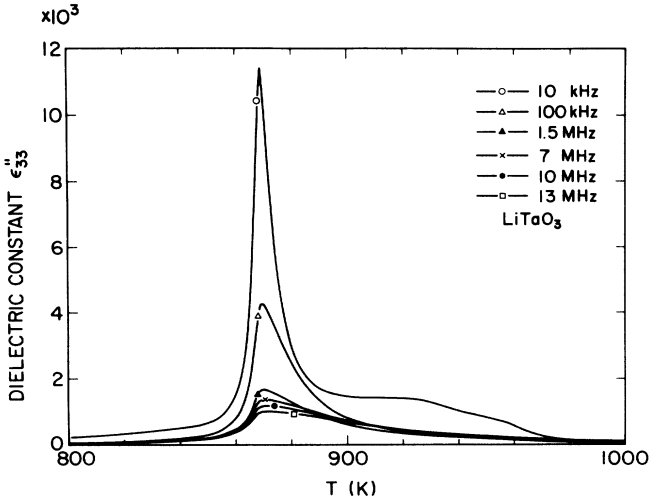

FIG. 8. Dielectric constant ϵ_{33}'' in $LiTaO_3$.

increasing temperature. As shown in Fig. 3(c), $\log_{10}\sigma_{11}$ in $LiTaO_3$ is proportional to $1/T$. This implies that $LiTaO_3$ possesses either a semiconductive or an ionic conductive character at high temperatures. Figure 8 indicates the imaginary part of dielectric constant ϵ_{33}'' in $LiTaO_3$, obtained from the anomalous part of σ_{33}. At T_C, ϵ_{33}'' increases with increasing frequency. Above 1000 K, ϵ_{33}'' becomes small and is practically independent of frequency. In contrast to ϵ_{33}'', the real part ϵ_{33}' has a frequency dependence up to 1200 K. Figure 9 shows a Cole-Cole plot obtained from the imaginary part ϵ_{33}'' versus the real part ϵ_{33}' at 880 K for $LiTaO_3$. The Cole-Cole plot in the frequency range up to 13 MHz cannot be described by the Debye relaxation equation. Thus the present results for ϵ_{33} deny the possibility that the phase-transition mechanism is of a pure order-disorder character.

In the SD $LiTaO_3$ crystal, Penna *et al.*[5,6] reported a diffusive central mode near T_C and the anomalous polariton dispersion above 660 K. They analyzed the central mode using the Debye relaxation equation and found that relaxation time τ near T_C is of the order of 5×10^{-12} s. Zhang and Scott[8] reported that relaxation time τ in Eq. (22) is 2.6×10^{-12} s at T_C. However, the dielectric

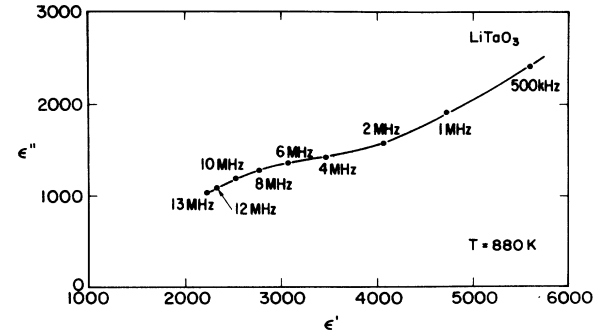

FIG. 9. Imaginary part vs real part of the dielectric constant as a function of frequency at 800 K in $LiTaO_3$ (Cole-Cole plot).

dispersion, observed in the frequency range between 10 kHz and 13 MHz, cannot be fitted by the Debye relaxation equation with τ of the order of 10^{-12} s.

Penna *et al.*[6] attributed the anomalous polariton dispersion to domain fluctuation below T_C. As indicated in Ref. 14, elastic-constant measurements clarify the distinction between SD and MD states just below T_C. Furthermore, dielectric dispersion exists in the PE phase of $LiTaO_3$. Consequently, the domain fluctuation model appears incompatible with the elastic-constant and dielectric-constant data.

According to Lines,[21] an anharmonic potential is responsible for the order-disorder character in Li ion distribution along the Z axis in these crystals. Both $q_{33}x_3P_3^2$ and $r_{333}x_3P_3^4$ are necessary to explain the temperature dependence of $C_{33}^P-C_{33}^E$ and $(\chi_{33}^x)^{-1}-(\chi_{33}^X)^{-1}$. Compared with $r_{333}x_3P_3^4$, the other components of rxP^4 appear to play a minor role in $C_{ii}^P-C_{ii}^E$ and $(\chi_{11}^x)^{-1}-(\chi_{11}^X)^{-1}$. Therefore, the dispersion of χ_{33} and the significance of $r_{333}x_3P_3^4$ may be interpreted in terms of the anharmonicity in the soft mode.

Figure 3(a) indicates that the anomaly in σ_{33} for $LiTaO_3$ is associated with the phase transition, because frequency-dependent conductivity σ_{33} exhibits a peak at T_C. The σ_{33} behavior may be related to the defects which become mobile near T_C. Halperin and Varma[22] discussed the influence of defects on susceptibility near a displacive phase transition and showed that the quantity δ^2 in Eq. (22) is proportional to the defect concentration. They predicted that the difference between the static and dynamic inverse susceptibility, caused by defects, would be practically independent of temperature. As shown in Fig. 2, the results for χ_{33}^{-1} above T_C appear consistent with the above prediction. The change in Curie temperature is related to the deviation from the stoichiometric composition.[15] The neutron scattering measurements[1,2] revealed that Li atoms above T_C occupy two equivalent positions on either side of the oxygen plane. Thus the coupling of the soft mode with vacancies or Li-ion motion may give rise to the dispersion. The coexistence of the soft mode and dispersion suggests that the phase transition in $LiTaO_3$ has an intermediate character between displacive and order-disorder categories.

Löhnert *et al.*[23] studied Mössbauer spectroscopy for the ^{181}Ta nucleus in $LiTaO_3$ and pointed out that a charge transfer from neighboring oxygen ions to the central Ta ion increases nonlinearly as a function of temperature. The dielectric dispersion may be influenced by a change in the electronic structure with increasing temperature.

In the PE phase of $LiNbO_3$, the difference in χ_{33}^{-1} between 1 and 13 MHz is considerably small,[10] as shown in Fig. 6(b). In view of this, the soft mode in $LiNbO_3$ may couple with the relaxation process weakly, compared with the soft mode in $LiTaO_3$.

V. CONCLUSIONS

Both the inverse-dielectric-susceptibility difference $(\chi_{ii}^x)^{-1}-(\chi_{ii}^X)^{-1}$ and the elastic-constant difference $C_{ii}^P-C_{ii}^E$ in $LiTaO_3$ have been interpreted consistently, in terms of both electrostrictive and higher-order interactions. The contribution of higher-order interactions to $(\chi_{33}^x)^{-1}-(\chi_{33}^X)^{-1}$ and $C_{33}^P-C_{33}^E$ appears to be attributed to the anharmonicity in the soft mode.

Both susceptibility χ_{33} and conductivity σ_{33} in $LiTaO_3$ exhibit a marked dispersion over the wide temperature range, including T_C. The coupling of the soft mode with vacancies or Li-ion motion may give rise to the dispersion. The results for χ_{33} and $C_{33}^P-C_{33}^E$ imply that the phase transition in $LiTaO_3$ has an intermediate character between displacive and order-disorder categories.

ACKNOWLEDGMENTS

We wish to thank Professor N. Kunitomi and Professor Y. Nakai (Osaka University) for valuable discussions and a critical reading of the manuscript. We are also grateful to Professor K. Hamano (Tokyo Institute of Technology), Dr. H. Unoki (Electrotechnical Laboratory), and Dr. M. Mori (Nagoya University) for stimulating discussions during the course of this work.

[1] S. C. Abrahams, E. Buehler, W. C. Hamilton, and S. J. Laplaca, J. Phys. Chem. Solids **34**, 521 (1973).
[2] E. J. Samuelsen and A. P. Grande, Z. Phys. B **24**, 207 (1976).
[3] M. R. Chowdhury, G. E. Peckham, and D. H. Saunderson, J. Phys. C **11**, 1671 (1978).
[4] W. D. Johnston, Jr. and I. P. Kaminow, Phys. Rev. **168**, 1045 (1968).
[5] A. F. Penna, A. Chaves, and S. P. S. Porto, Solid State Commun. **19**, 491 (1976).
[6] A. F. Penna, S. P. S. Porto, and E. Wiener-Avnear, Solid State Commun. **23**, 377 (1976).
[7] K. A. Müller, Y. Luspin, J. L. Servoin, and F. Gervais, J. Phys (Paris) Lett. **43**, L-537 (1982).
[8] M. Zhang and J. F. Scott, Phys. Rev. B **34**, 1880 (1986).
[9] Y. Okamoto, P. Wang, and J. F. Scott, Phys. Rev. B **32**, 6787 (1985).
[10] I. Tomeno and S. Matsumura, J. Phys. Soc. Jpn. **56**, 163 (1987).
[11] A. M. Glass, Phys. Rev. **172**, 564 (1968).
[12] T. Yamada, H. Iwasaki, and N. Niizeki, Jpn. J. Appl. Phys. **8**, 1127 (1969).
[13] C. Prieto, L. Arizmendi, J. A. Gonzalo, F. Jaque, and F. Agullo-Lopez, Phys. Rev. B **34**, 7396 (1985); C. Prieto and J. A. Gonzalo, Solid State Commun. **61**, 437 (1987).
[14] I. Tomeno, J. Phys. Soc. Jpn. **51**, 2891 (1982).
[15] R. L. Barns and J. R. Carruthers, J. Appl. Cryst. **3**, 395 (1970).
[16] A. W. Warner, M. Onoe, and G. A. Coquin, J. Acoust. Soc. Am. **42**, 1223 (1967).
[17] W. Rehwald, Adv. Phys. **22**, 721 (1973).
[18] H. Iwasaki, H. Toyoda, and H. Kubota, Jpn. J. Appl. Phys. **6**,

1338 (1967).
[19]A. S. Barker, Jr., A. A. Ballman, and J. A. Ditzenberger, Phys. Rev. B **2**, 4233 (1970).
[20]I. P. Kaminow and W. D. Johnston, Jr., Phys. Rev. **160**, 519 (1967).
[21]M. E. Lines, Solid State Commun. **10**, 793 (1972).
[22]B. I. Halperin and C. M. Varma, Phys. Rev. B **14**, 4030 (1976).
[23]M. Löhnert, G. Kaindl, G. Wortmann, and D. Salomon, Phys. Rev. Lett. **47**, 194 (1981).